Supplemental Data. Smertenko et al. (2008) The C-terminal variable region specifies the dynamic properties of Arabidopsis Microtubule-Associated Protein MAP65 isotypes.

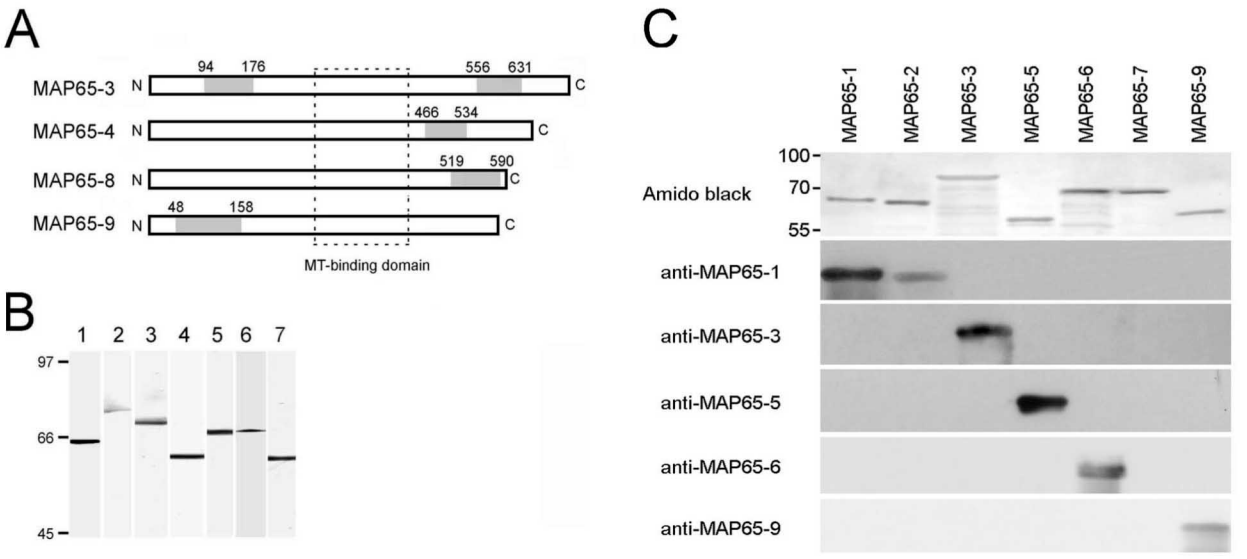

Supplemental Figure 1. Characterisation of antibodies against the MAP65 isotypes.

A. Diagram shows the regions (grey-shadowed) of MAP65-3, -4, -8 and –9 used for raising the antibodies. A broken line indicates the conserved microtubule-binding domain.

B. Western blotting of a total protein extract from *A. thaliana* tissue culture cells with anti MAP65-1 (lane 1), MAP65-3 N-terminal fragment (lane 2), MAP65-4 (lane 3), MAP65-5 (lane 4), MAP65-6 (lane 5), MAP65-8 (lane 6) and MAP65-9 (lane7). Each antibody cross-reacted with a distinct band in the total protein extract.

C. Western blotting of the recombinant MAP65 isotypes with the same panel of antibodies as in panel B. Amido Black staining shows total amount of loaded proteins on the nitrocellulose membrane, bars and numbers on the left hand side of the image indicate position and size of the specific molecular weight markers. Anti MAP65-1 cross-reacted with MAP65-2, while the rest of the antibodies recognised the corresponding recombinant protein. Anti MAP65-4 and MAP65-8 did not cross-react with any of the recombinant proteins used here and therefore were not included in the figure.

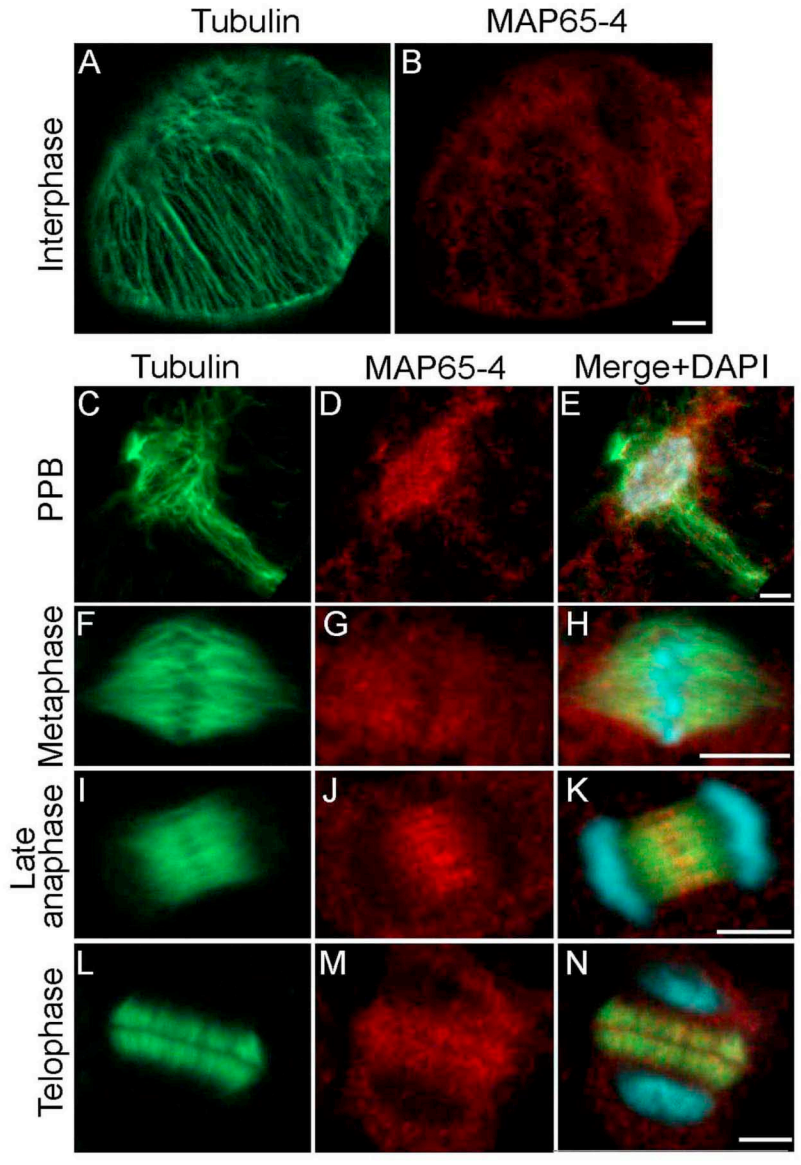

Supplemental Figure 2. Immunolocalisation of MAP65-4 in microtubule arrays of *A. thaliana* tissue culture cells. Nuclei are stained with DAPI and shown in blue on the merged images.

A,B, Images show no association of MAP65-4 with cortical microtubules in interphase cells.

C-E, Co-localisation of MAP65-4 with microtubules in the pre-prophase band during late G2 phase. Most of the signal accumulates around the nucleus where there is a meshwork of microtubules.

F-H, Images show a very weak MAP65-4 signal in the region of the mitotic spindle.

I-K, MAP65-4 staining accumulates in the midzone during late anaphase.

L-N, Most of the MAP65-4 staining during the later stages of phragmoplast development localises mostly on the microtubules, with some visible in the midzone.

Scale bar, 5 μm.

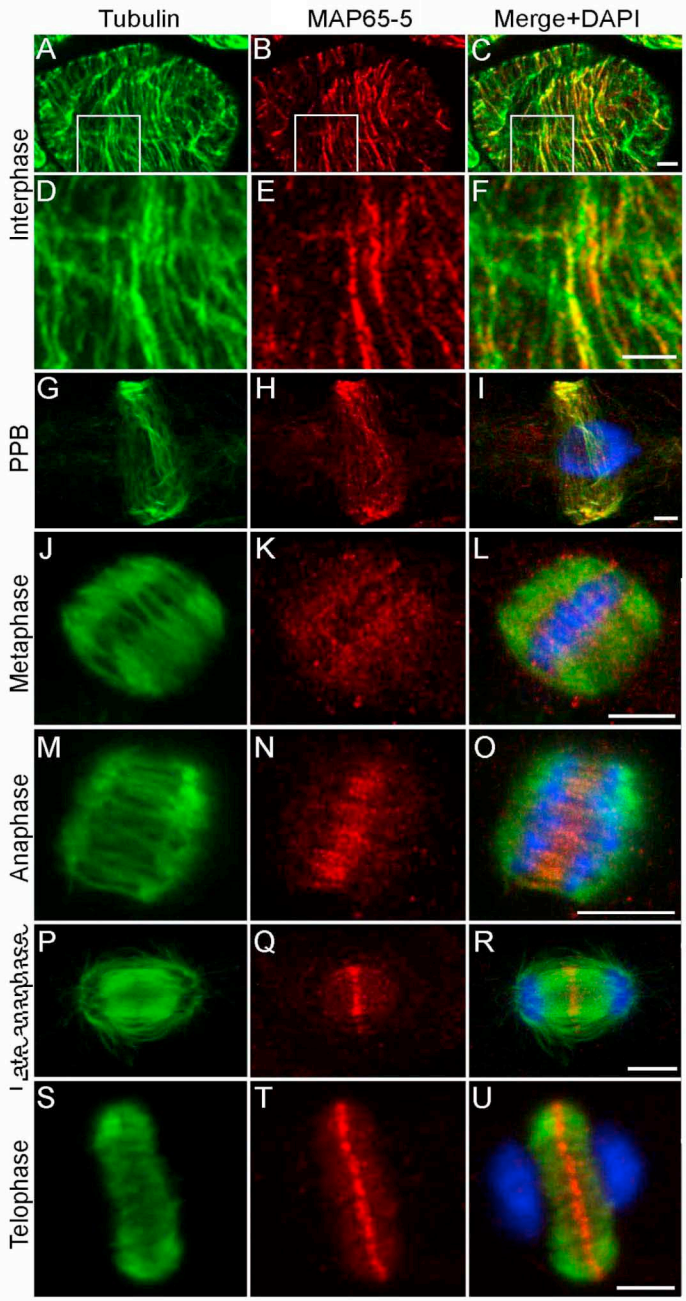

Supplemental Figure 3. Immunolocalisation of MAP65-5 in microtubule arrays of *A. thaliana* tissue culture cells.

A-C, Images show MAP65-5 staining in the interphase cortical microtubule array;

D-E, Higher magnification of the area outlined in A-C showing association of MAP65-5 with a subset of cortical microtubules;

G-I, Preprophase band labelled by MAP65-5 staining.

J-L, Metaphase spindle with a diffuse co-localisation of MAP65-5 with spindle microtubules.

M-O, Anaphase spindle. MAP65-5 accumulates at the spindle midzone.

P-R, Late anaphase, MAP65-5 concentrates at the midzone.

S-U, Late stage of telophase. MAP65-5 still concentrates in the phragmoplast midzone.

Scale bar, 5 μm.

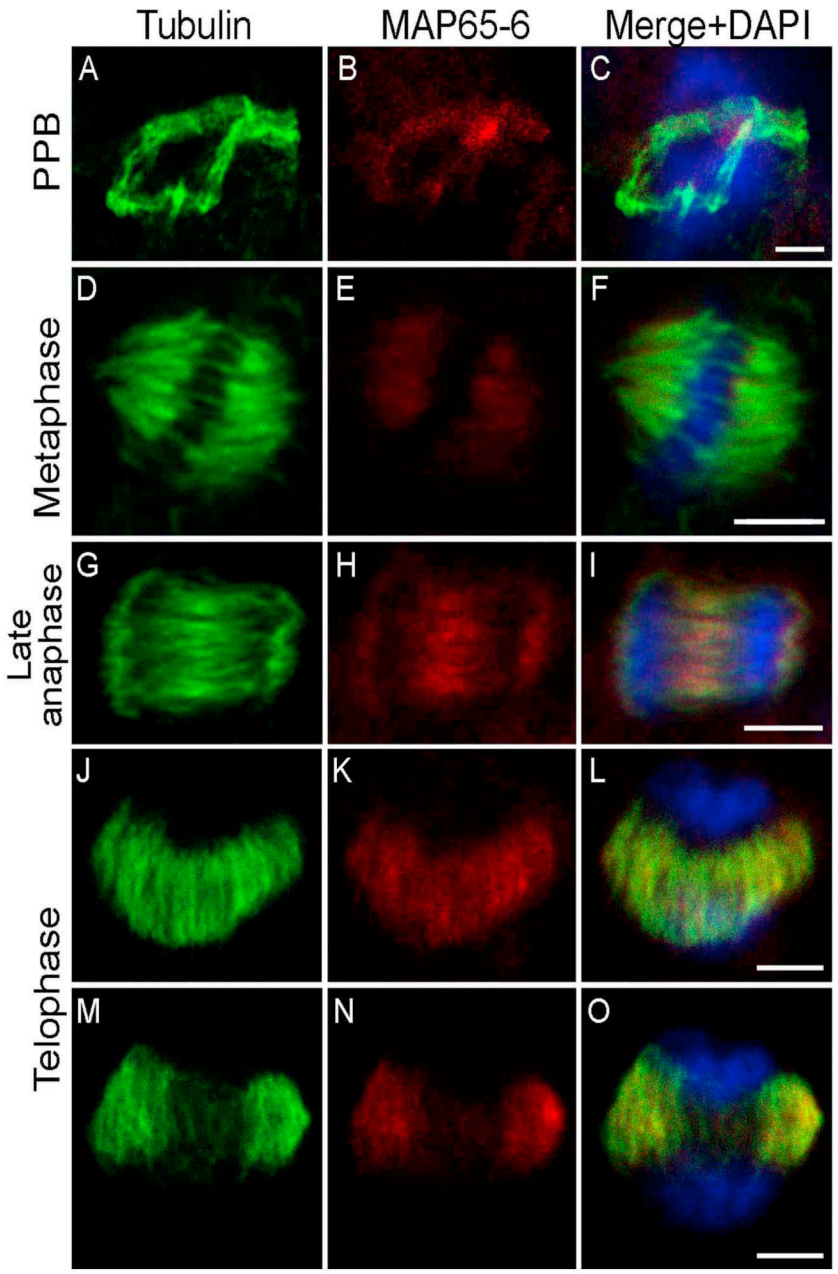

Supplemental Figure 4. Immunolocalisation of MAP65-6 in microtubule arrays of *A. thaliana* tissue culture cells.

A-C, Pre-prophase band microtubules are bound by MAP65-6.

D-F, Mitotic spindle microtubules have no obvious binding by MAP65-6.

G-I, MAP65-6 localises to the anaphase spindle midzone.

J-L, Maximal projection of several confocal sections showing half of a phragmoplast. MAP65-6 binds to the microtubules but does not accumulate in the midzone.

M-O, Single confocal section through the centre of the same phragmoplast shown in L-N, Concentration of MAP65-6 in the phragmoplast midzone was observed at the expanding edge.

Scale bar, 5 μm.

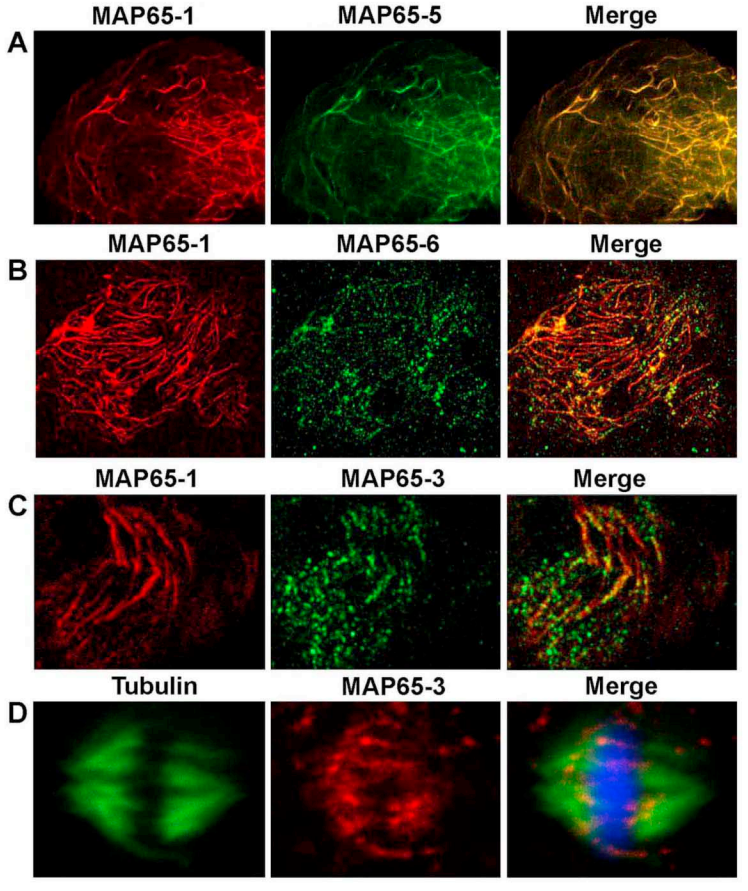

Supplemental Figure 5. Immunolocalisation of MAP65 isotypes in *A. thaliana* protoplasts and tissue culture cells.

A, MAP65-1 and MAP65-5 bind to the same sub-set of cortical microtubules.

B, Co-localisation of MAP65-1 and MAP65-6. Most of the MAP65-6 punctate staining is located along cortical microtubules which are also decorated with MAP65-1.

C, MAP65-3 localises to some cortical microtubules decorated with MAP65-1 with the punctate staining pattern similar to MAP65-6.

D, MAP65-3 binds to the fragments of microtubules in the metaphase spindle.

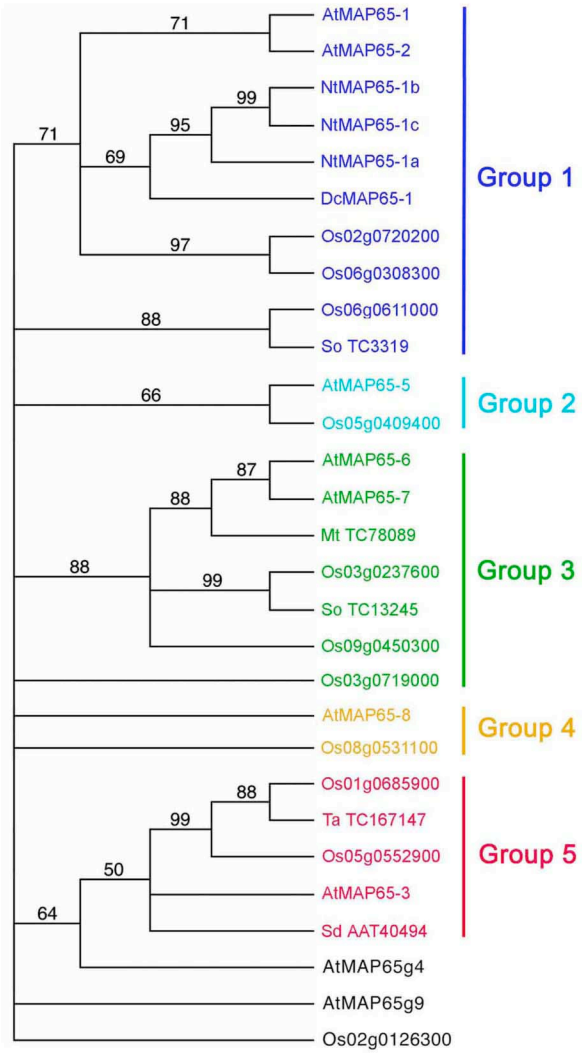

Supplemental Figure 6. Phylodendrogram of MTB2 regions of MAP65 genes shown in Figure 1 demonstrates conservation of MTB2. The sequences were aligned and the tree constructed as described in the Methods section and rooted using MTB2 sequence of Os02g0126300, except that the bootstrap value cut off point was set at 50%. The five main groups defined using full length sequences are preserved, apart of group 4, which now is split in two independent branches. Two members of Group 1 (one from rice and one from sugar cane) and one of Group 3 (rice) appear as independent branches on the tree. These MTB2 regions have obviously diverged after the split between monocotyledons and dicotyledons. It also indicates that other parts of the proteins are playing a role in determining the structure of the phylodendrogram shown in Figure 1. Letters at the beginning of each protein name indicate the species as listed below: At – *Arabidopsis thaliana*, Dc – *Daucus carota*, Mt – *Medicago truncatula,* Nt – *Nicotiana tabacum*, Os – *Oryza sativa*, So – *Saccharum officinarum*, Ta – *Triticum aestivum*, Sd – *Solanum demissum.* Numbers represent Genebank accession numbers.

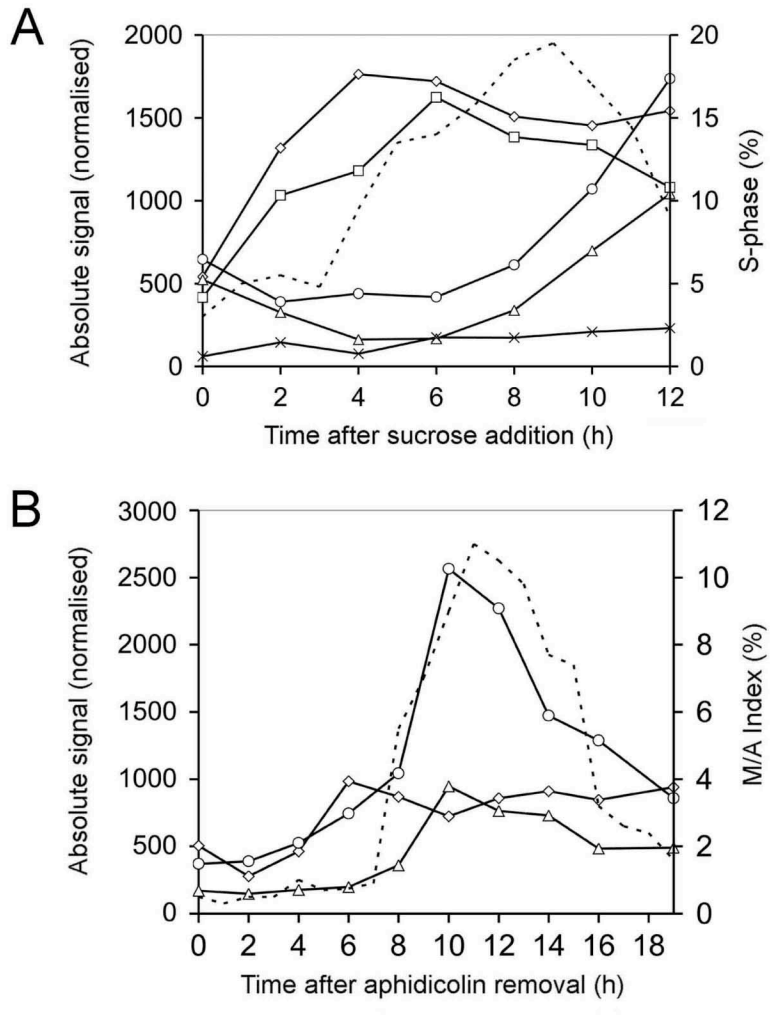

Supplemental Figure 7. Cell cycle dependent changes in the levels of MAP65 gene transcription.

The graphs only represent transcription profiles for the genes that exhibit statistically significant changes above the background level.

A. Cells re-enter the cell cycle after sucrose starvation and this synchronises the cells in G1. The broken line shows the percentage of cells in S-phase. MAP65-2 and MAP65-5 are up-regulated in G1, while the transcription level of MAP65-3, MAP65-4 and MAP65-8 rises towards S-phase.

B. Synchronisation of cells in S-phase using the DNA synthesis inhibitor aphidicolin. The broken line indicates the percentage of cells in M-phase. MAP65-2, MAP65-3 and MAP65-4 are up-regulated upon M-phase entry. In agreement with this observation, immunolocalisation of MAP65-3 and MAP65-4 in interphase cells showed weak or non-detectable association with microtubules.

MAP65-2 (diamonds), MAP65-3 (triangles), MAP65-4 (circles), MAP65-5 (open squares), MAP65-8 (crosses).

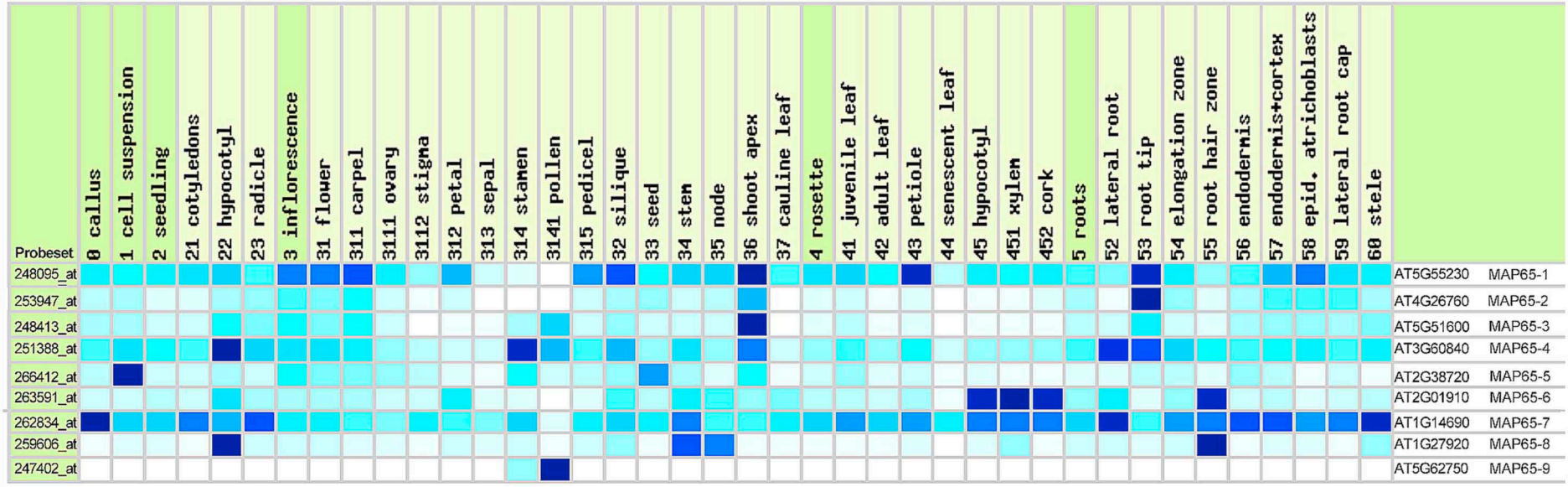

Supplemental Figure 8. Transcription of MAP65 genes in tissues and organs of *A. thaliana* plants. The analysis of Affymetrix microarray data was carried out using the Genevestigator website. The colouring of the cells in the table represents the level of transcription with the darker colouring indicating a higher level of transcription. This figure shows simultaneous transcription of several isotypes in each tissue or organ and demonstrates that MAP65-1, MAP65-4 and MAP65-7 are ubiquitous, while the transcription of other genes prevails in some tissues/organs.

Supplemental Table 1. Characteristics of Arabidopsis MAP65 protein sequences.

Gene name	Accession Number	No. AA	Mr	pI	C-ter AA	C-term. pI	N-term. pI
MAP64-1	At5g55230	587	65.8	4.97	484-587	10.55	4.71
MAP65-2	At4g26760	578	65.2	5.02	484-578	10.20	4.81
MAP65-3	At5g51600	707	80.3	5.75	485-707	10.22	5.03
MAP65-4	At3g60840	648	73.4	7.19	452-648	9.93	5.36
MAP65-5	At2g38720	550	62.3	6.22	476-550	10.14	5.49
MAP65-6	At2g01910	608	69.4	6.87	494-608	10.21	5.73
MAP65-7	At1g14690	603	69.1	6.30	494-603	10.00	5.67
MAP65-8	At1g27920	592	68.3	8.41	520-592	10.97	6.45
MAP65-9	At5g62750	549	63.9	5.20	487-549	10.53	4.91

Supplemental Table 2. Standard deviation of the signal generated by mRNA probes prepared from Arabidopsis tissues with MAP65 spots on 22k *A. thaliana* Affymetrix gene chip (the graphical representation of the data is shown in Supplemental Figure 8).

Gene name	Accession Number	Deviation
MAP65-1	At5g55230	0.39
MAP65-2	At4g26760	0.82
MAP65-3	At5g51600	0.76
MAP65-4	At3g60840	0.43
MAP65-5	At2g38720	0.76
MAP65-6	At2g01910	0.76
MAP65-7	At1g14690	0.31
MAP65-8	At1g27920	1.15
MAP65-9	At5g62750	4.65

Supplemental Table 3. Primers used in this study.

Primers for expression of full-length recombinant MAP65 proteins	
AtMAP54-2	
Forward	ACATATGGCAGTGACAGAAGCAGAAAATCC
Reverse	TGTCGACTCACGGTGAAGCCATCACTGGGTCAG
AtMAP54-3	
Forward	ACATATGGCTAGCGTGCAGAAAGATCCGATTCTTCAAGTAGAGACA
Reverse	TCTCGAGTCATCTTCTCTTCTTCCAA6GTCCTG
AtMAP54-5	
Forward	GCTAGCATGTCTCCGTCTTCAACCAC
Reverse	GGATCCTCAAGCTATGCATCCAACGCG
AtMAP54-6	
Forward	AACATATGCTGGAAATTGGA
Reverse	TTCTCGAGTCAGCCTTGGAG
AtMAP54-7	
Forward	ACATATGCTGGAGATTGAAAGCCCTACGAG
Reverse	TCTCGAGTTAGTTATATAACGGTGAATCTGGTTCAGAGCC
AtMAP54-9	
Forward	ACATATGTCCAAATCTCAAATCGAATCAAC
Reverse	TCTCGAGTCAGCCATGGCGTGATAGAGGAG
Primers for expression of fragments for antibody preparation	
AtMAP65-3	
Forward	ACATATGTCTGATCAAAGCGTTGGGAGC
Reverse	TCTCGAGTTACTCCTTCTGAAGTACTTGCAG
AtMAP65-4	
Forward	ACATATGTATGGGTCTAAACCAAGCCCA
Reverse	CTCGAGTTATGAAAGAGTTGGAAGAGCTGAA
AtMAP65-8	
Forward	ACATATGAAGAAGATGAGCATTCCAC
Reverse	ACTCGAGTTACTTTCTGCTTTCTCTTCTTATAG
AtMAP65-9	
Forward	ACATATGCGAAAAATCGAAAAGGTTAAAGA
Reverse	ACTCGAGTTATTCATCAGCAGAAAAATCAGATG